

# Motion tracking and analysis system for magnetotactic bacteria

Martin Mankiewicz and Sylvain Martel\*

NanoRobotics Laboratory, Department of Computer Engineering and Institute of Biomedical Engineering, École Polytechnique de Montréal (EPM), Campus of the Université de Montréal, P.O. Box 6079 Station Centre-Ville, Montréal, Québec H3C 3A7, Canada.

## ABSTRACT

The possibility to conceive a nanorobot propelled by flagellated magnetotactic bacteria is becoming a reality. But the development of such complex systems requires the implementation of various functionalities, one of which being the tracking of such devices with sufficient speed and accuracy. In this paper, we present an automated tracking system developed with modern computational and microscopy equipment designed to follow a bacterium through various swimming paths. The results obtained with such system are presented in order to assess the platform real-time performance in tracking MC-1 magnetotactic bacteria. This system is also used to record data related to the movement of the bacteria which may prove to be useful in other field of research besides nanorobotics.

**Keywords:** Computer-vision, micro-bio-actuator, optical microscope tracking, magnetotactic bacteria

## 1. INTRODUCTION

In the field of nanotechnology and especially in interventional nanomedicine, the use of flagellated bacteria and in particular Magnetotactic Bacteria (MTB) has been proposed to act as propulsion engines and steering for microscopic robots for operations such as targeting tumors<sup>1</sup>. The possibility of controlling different parameters of these biological entities becomes attractive to engineers and scientists. Several parameters need to be controlled before such bio-actuation mechanism becomes really useful for micro-robots.

Experimental results demonstrating the use of MTB for controlled micro-actuation of moving microscopic objects including micro-robots in aqueous medium have been published<sup>2,3</sup>. It was also shown that the swimming direction of these MTB could be modified by applying a torque from a directional magnetic field to the chain of magnetosomes (membrane-based nanoparticles) embedded in each bacterium. These results showed that these MTB have great potential not only in the development of new types of micro-robots but also in the conception of new Micro-Electro-Mechanical-Systems (MEMS).

As such, specially developed experimental platforms and more specifically tracking platforms capable of recording useful data to guide in the design of such new type of micro-robots are critical for the success of this project.

## 2. MATERIAL AND METHODS

### 2.1 Architecture and configuration

In microbiology, the use of optical microscopy has proven to be an effective way of studying bacteria and small organisms in their natural environment<sup>4</sup>. With the development of integrated CCD cameras, automatic servo-controlled focus and motorized stages, these machines now have powerful new means of operation. Adding the ever increasing computational possibilities of modern CPUs and graphic cards makes possible the development of completely automated analysis and microbiology study platforms.

---

\* [sylvain.martel@polymtl.ca](mailto:sylvain.martel@polymtl.ca); Phone: 1 514 340-4711 ext.5098; Fax: 1 514 340-5280; [www.nano.polymtl.ca](http://www.nano.polymtl.ca)

To track and detect the bacteria, custom software has been programmed and linked to a Zeiss Axio Imager Z1 optical microscope. Images are acquired with an AxioCam MRm black and white camera using DarkField 400× reflection mode microscopy. Video transfers are done through an IEEE-1394 (FireWire) communication link with a maximum transmission rate of 400 Mb/s. The Zeiss robotic scanning stages being part of the microscope platform is used for robotic autonomous displacement of the sample.

The tracking and analysis software was developed as a Visual Basic Application (VBA) for the AxioVision Release 4.5 program. The image acquisition was realized using Carl Zeiss image acquisition functions and post processing and analysis were built as custom software developed in-house. Tests were realized on an Intel Pentium 4, 3.0 GHz processor with 2.87 Go of RAM running Microsoft Windows XP. The computer was equipped as well with an ASUS Extreme AX800 XL graphic card.

For the experiments, MC-1 magnetotactic bacteria were used. The bacteria (~2 μm in diameter) were attached to Sulfate FluoSpheres microbeads (2% solids from Invitrogen) using an antibody developed in our laboratory. Bacteria motility and characterization were tested by using our custom tracking and analysis software depicted in Fig. 1.

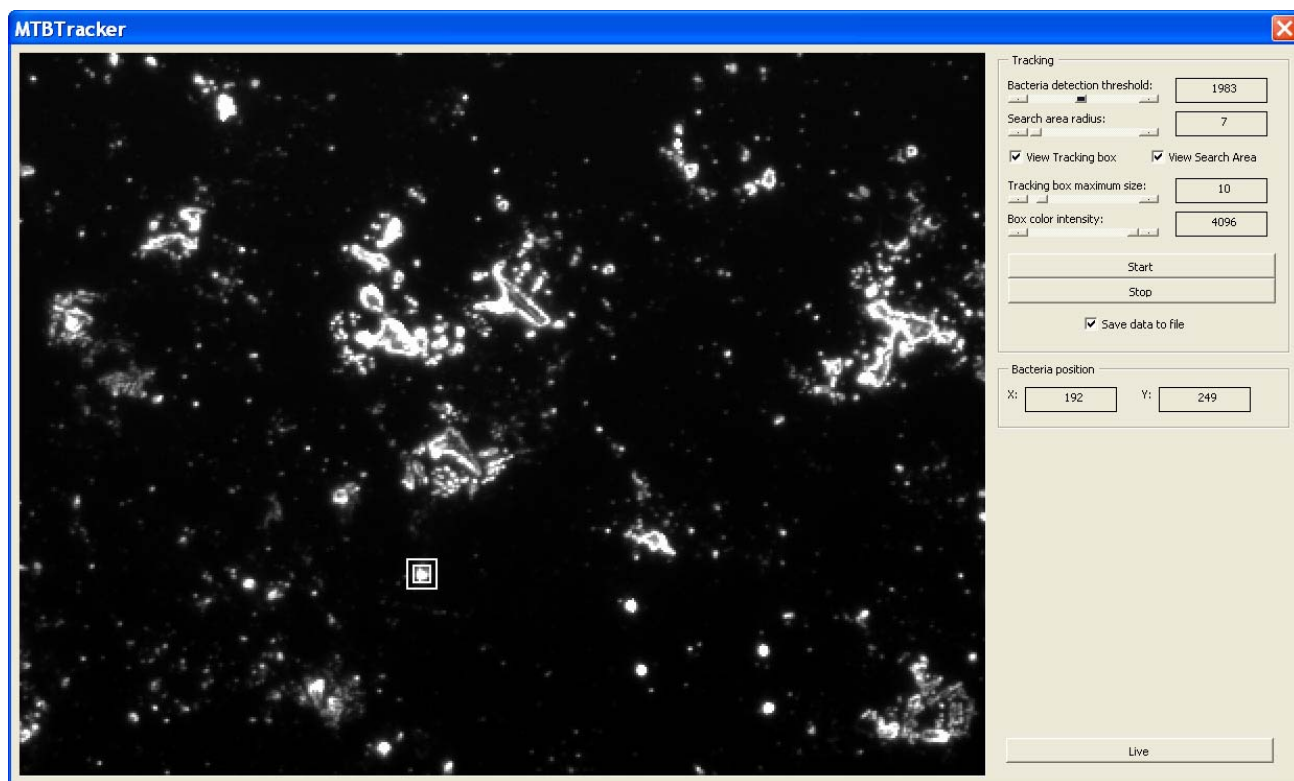


Fig.1 The MTBTracker software user interface. The bacteria detection threshold shows the pixel intensity value used for the correct delimitation of the tracked bacterium contour. The search area radius presents the number of pixels of the half outer rectangular box used for tracking the bacterium. Tracking box maximum size limits the size of the smaller rectangular box delimiting the bacterium contour. Different box intensities are used to get a better contrast of the tracking boxes from the background display.

The platform makes possible real-time tracking of a bacterium attached to a bead with an average refresh rate of 10 frames per second (fps). The user interface offers simple configuration of the *bacteria detection threshold*, *search area dimension*, *tracking box maximum size* as well as *box color intensity*. The user is able to begin the tracking by clicking on the bacterium in the live display window or by using the start button. The *view tracking box* and *view search area* check boxes are used to display or not in the live window the rectangular tracking limits. Those parameters can be turned off to improve computational performance. The *save data* check box is used to activate or deactivate data recording

concerning bacteria position and timestamps. The *bacteria position* window displays the bacterium current position in pixels.

## 2.2 Tracking algorithm

The tracking algorithm used for this application is an adaptation of the region growing segmentation technique. The software is executed in real-time on each frame acquired by the CCD camera mounted on the microscope. In an effort to maximize the efficiency of the system, fine tuning and calibration is set by the user in the graphic interface in order to facilitate adjustment to various lighting conditions. Any modification made to the parameters described earlier instantly impacts the code execution.

The algorithm is launched as a callback method executed every time an image is acquired by the camera. Two control paths are then possible. First path is run through if the pixel color intensity of the center of the tracking zone is higher than the *bacteria detection threshold* limit, meaning a bacterium is located in the center of the search area tracking box. The second path is run through if no bacterium is detected and consequently the algorithm searches for a bacterium in the search area box.

If a bacterium is located in the center of the detection zone, the algorithm will grow respectively one pixel layer at a time on the top, bottom left and right sides of the borders increasing the tracking box size accordingly. The algorithm grows until all borders are constituted of pixels with intensities lower than the *bacteria detection threshold* value. Once the tracking box is done growing, the bacterium center is attributed to the center of that zone. Figure 2 presents the different tracking steps of the algorithm.

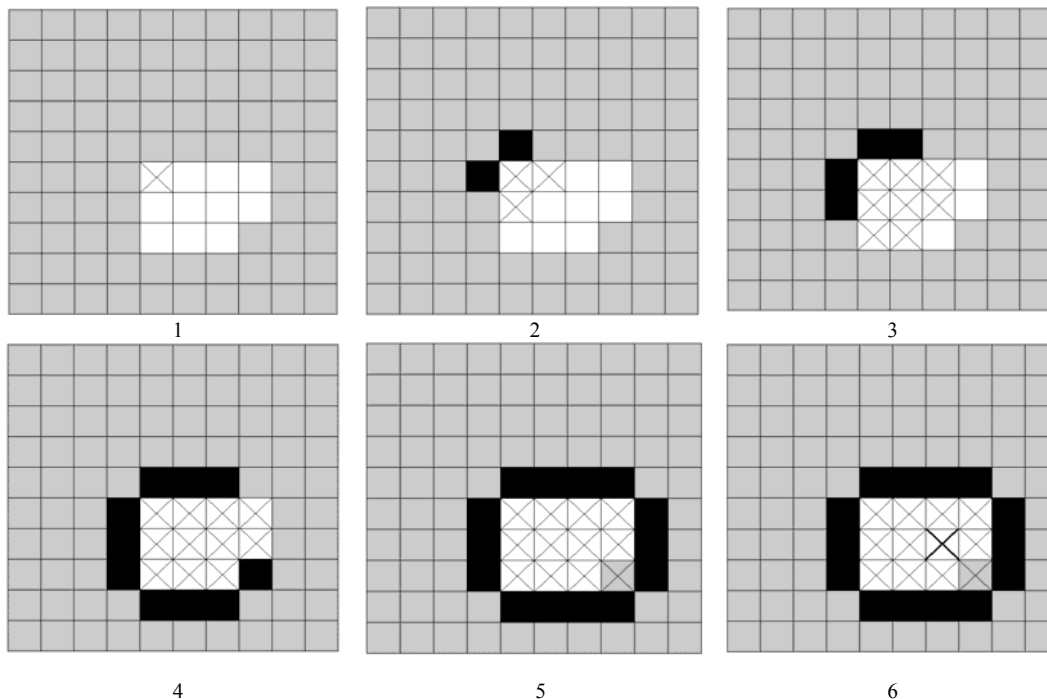


Fig.2 Bacterium border detection algorithm. The process starts in the top left corner with a border of 1(x) by 1(y) pixel, ending in the bottom right corner with a border of 4(x) by 3(y) pixels.

The second path that the algorithm can run through is the one searching for a bacterium in the search area. The user sets the size of this area using the *search area dimension* parameter. The section of the algorithm, similarly to its previous part implements an adaptation of the region growing algorithm. The algorithm will seek for a bacterium in the delimited zone until it finds one. If no bacterium is found, the algorithm loops until a new region is chosen by the user or until a bacterium passes in the tracking zone, as presented in Fig. 3.

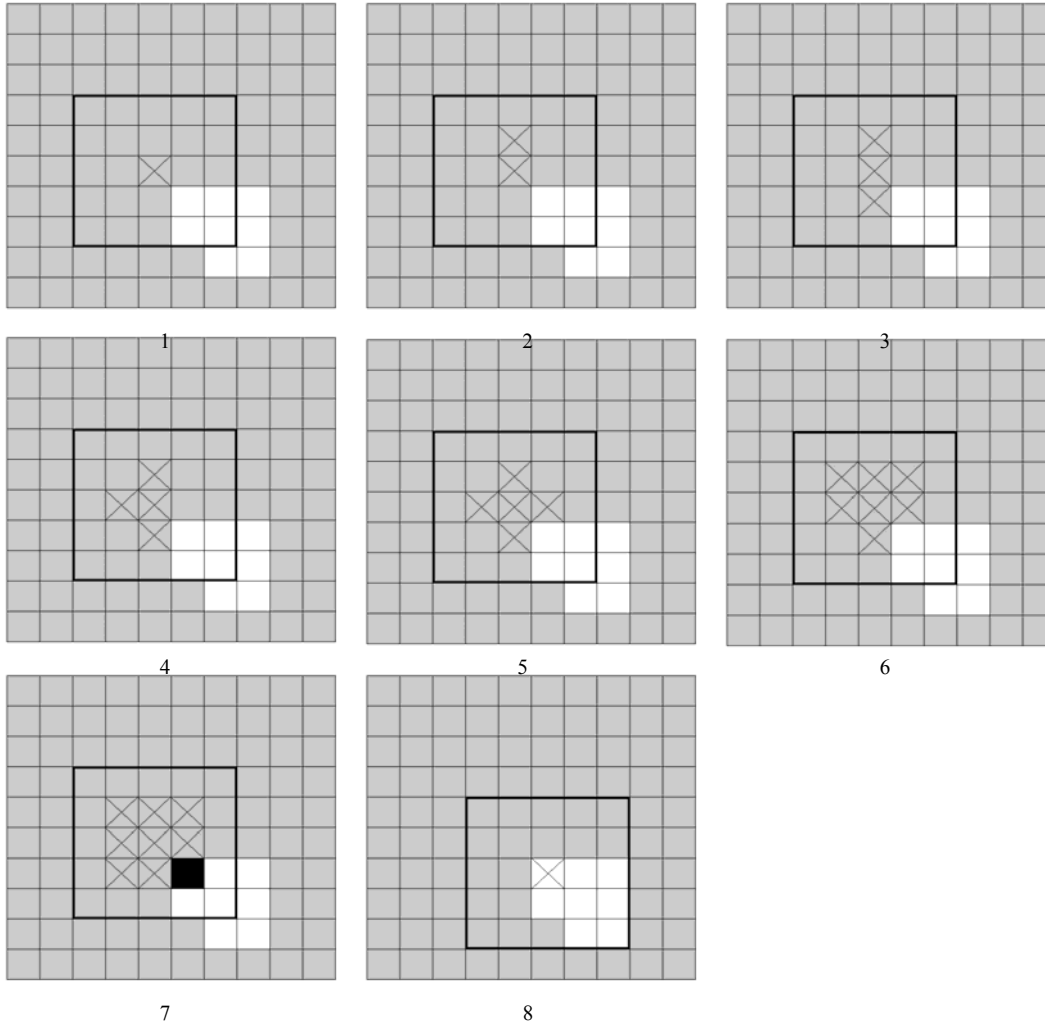


Fig. 3 Bacterium search algorithm. Grids 1 to 5 present the process of one loop of the tracking procedure. The second loop starts on grid 6 and ends on grid 7 when a bacterium is found. Search area center is adjusted and the first part (Fig.2) of the algorithm is then launched.

Problems of synchronization can arise when the search area algorithm requires more processing time than the camera acquisition rate. To avoid launching multiple bacteria search algorithms on different acquired images, the system has been conceived using semaphores to ensure that only one process runs at a time. Frames received when the algorithm is not done performing are dropped. The algorithm consequently always starts analyzing the newest image received. Statistics on the system performance affected by the search area range are presented in the next section.

### 3. RESULTS

#### 3.1 System characterization

Analysis of the system performance was realized on a bacteria free slide. The bacteria detection threshold parameter was set to the maximum value of 4096. This configuration ensures that only the second part of the algorithm is executed giving us consistent results throughout the tests with different search area sizes. Test results were saved in a text file presenting the *search area dimension* value and the timestamp at which the value had been recorded. The graphic in Fig. 4 shows our results.

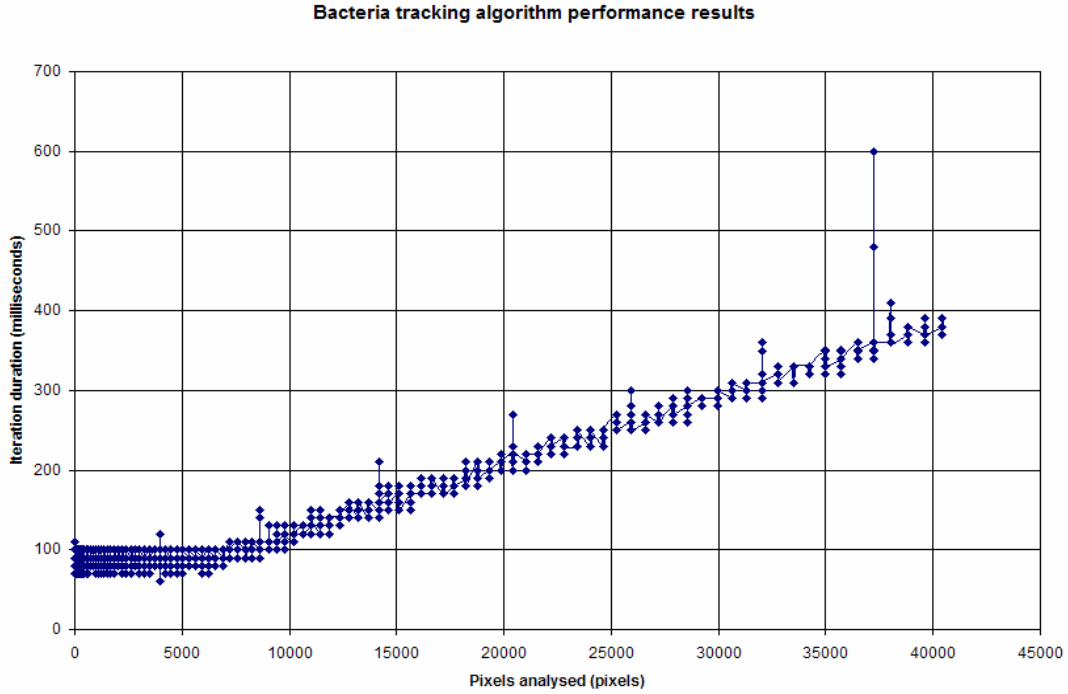


Fig. 4 Performance results of the bacterium tracking algorithm. The x axis presents the number of pixels tested on bacterium detection with negative results. The y axis presents the time delay between two iteration of the tracking algorithm.

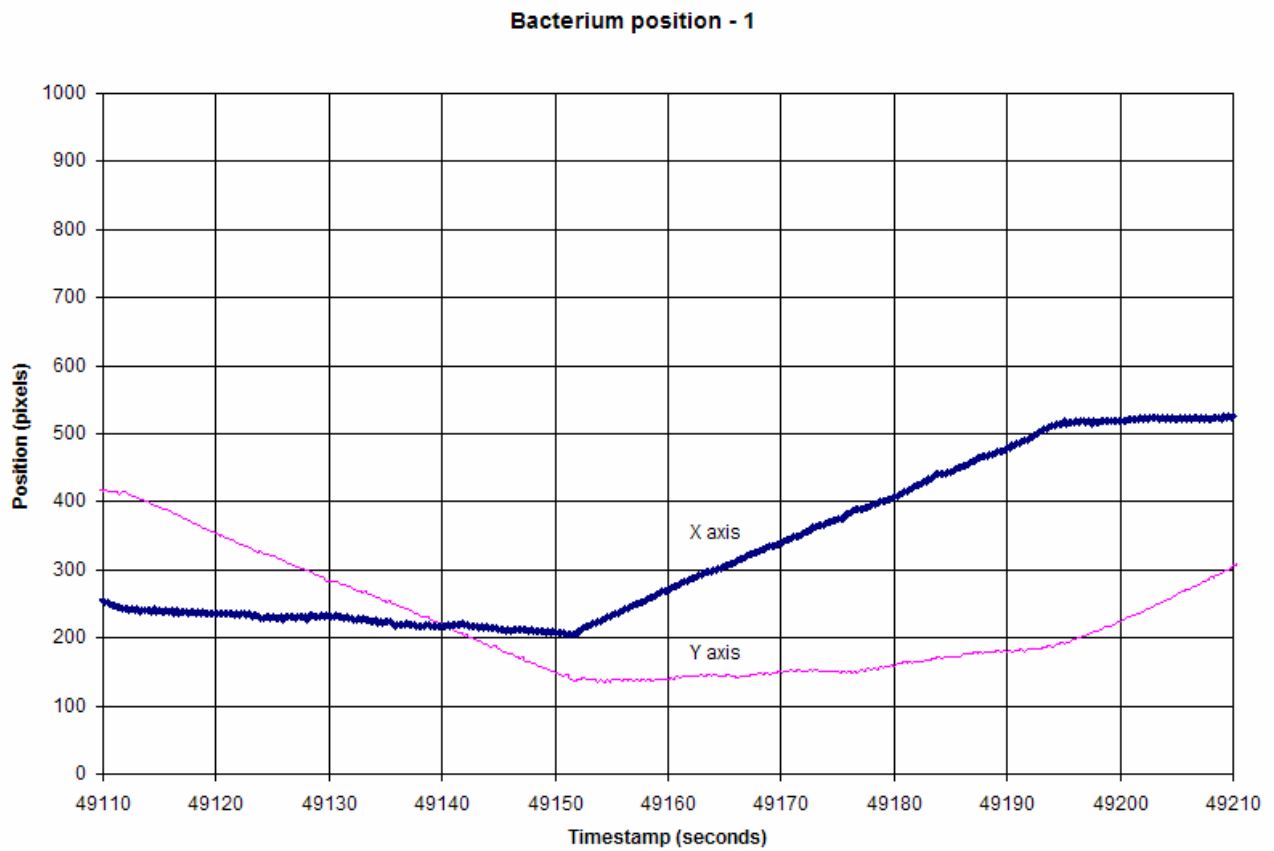
The second part of the characterization tests were done to get results on the relation between the maximum tracking speed and the object/search area ratio. Tests were performed using a microscope slide presenting a white dot of  $11 \times 11$  pixels corresponding to a *search area radius* of 5. The *search area radius* parameter corresponds to half the tracking box length minus one pixel. The system was launched to track the dot which was then moved with the motorized stages. The speed of the stages was controlled with the Zeiss AxioVision application. The stage was set to move forward and backward at different speeds increasingly until the tracking would be lost. In the end, only the results presenting a constant speed over a minimum of 15 readings were conserved. Data were recorded in a file where we could read the timestamp at which the data had been saved and the pixel coordinates of the center of the tracked dot. The speed was calculated by derivation of the position over time. Images were acquired with a ratio of 0.62 micrometer per pixel. Table 1 displays test results of tracking speed characterization.

Table1. Test results for different configurations of tracking parameters

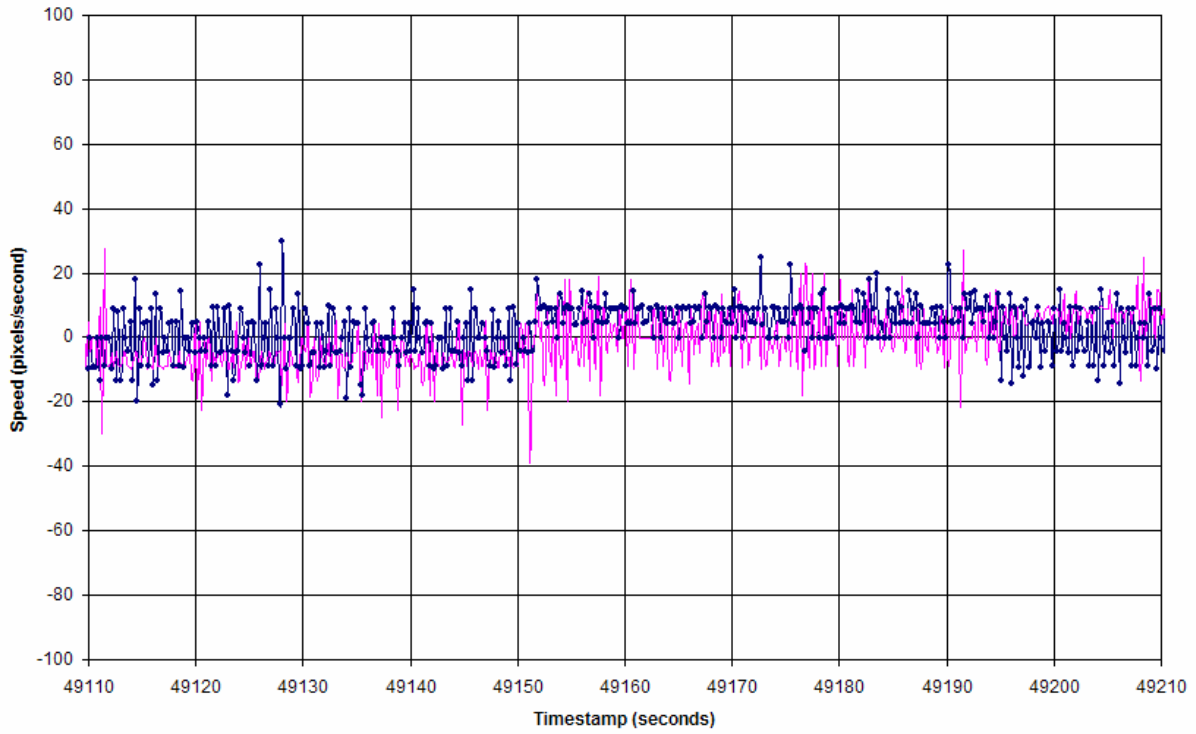
Tracked object size (pixels)	Search Area Radius (pixels)	Object/Area Ratio (%)	Maximum Speed Recorded (pixels/second)
121	3721 (30)	3.25	117.55
121	2601 (25)	4.65	116.24
121	1681 (20)	7.19	112.62
121	961 (15)	12.59	51.07
121	441 (10)	27.44	49.89
121	121 (5)	100.00	27.33

### 3.2 Bacteria tracking

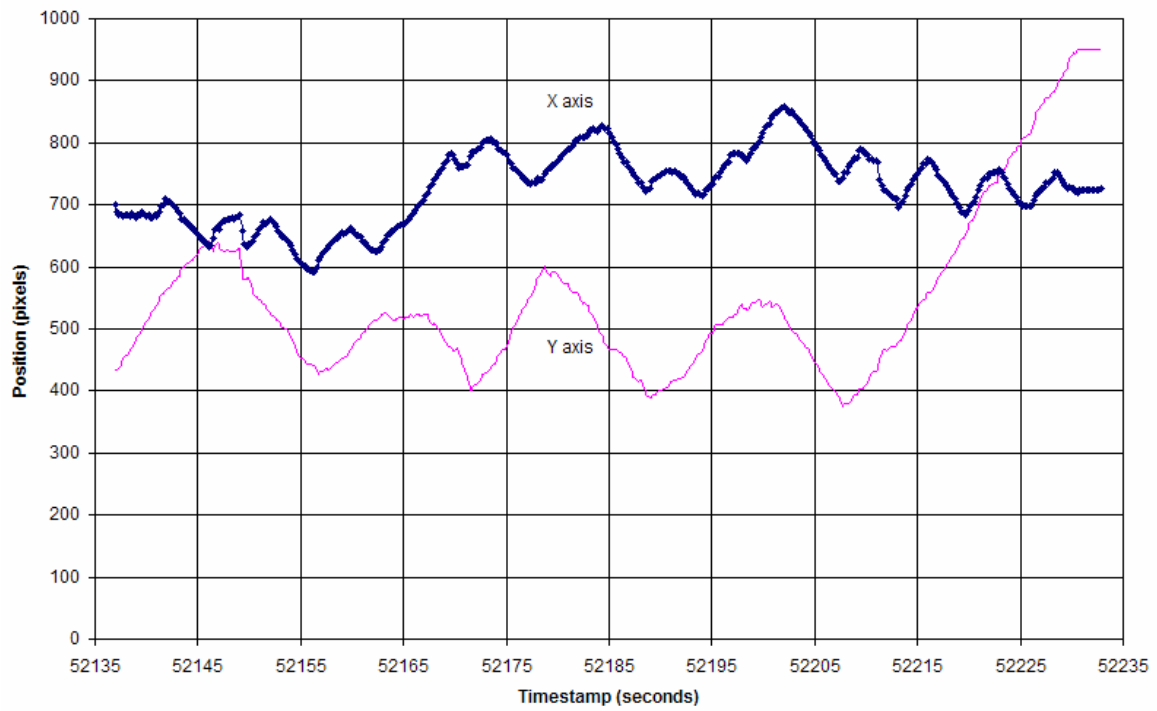
Two tracking tests were performed on the MC-1 magnetotactic bacteria. The first one tracked a bacterium attached to a 6.2 micrometer bead using a 20×/0.40HD microscope objective and the second one using a 50×/0.50HD objective. The window ratio for the first test presented a 0.51 micrometer/pixel ratio and a 0.21 micrometer/pixel ratio in the second test. *Search area radius* was set to 30 in both tests with a tracked object of size 10 giving us a ratio of 11.8%. *Detection threshold* in the lighting context was optimized for a value of 130. Tests were done on a 1388×1040 pixels window presenting a 16-bit grey level display. Figure 5 is a graphical representation of the outcome of tests.



**Bacterium speed - 1**



**Bacterium position - 2**



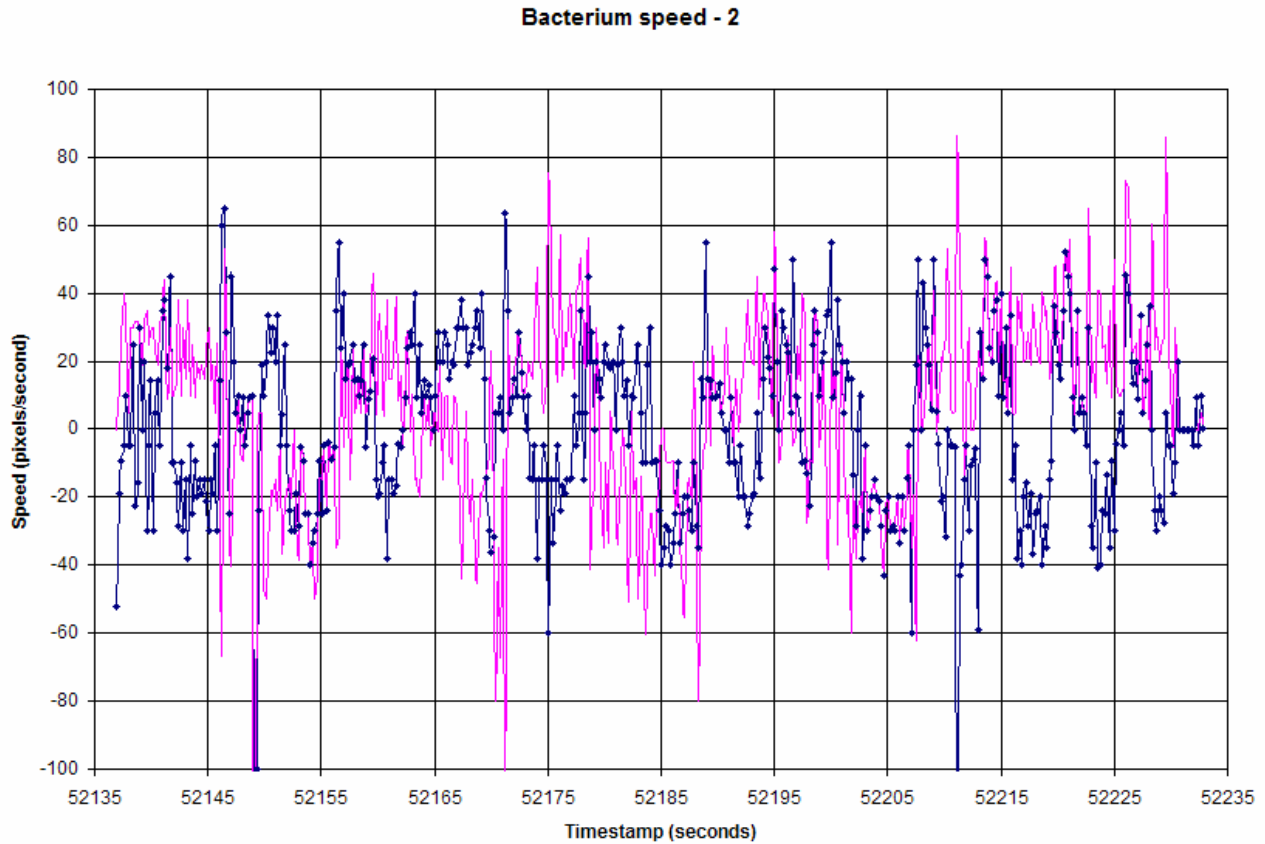


Fig. 5 Graphics of the MTB tracking test results. Dark-dotted line presents the X axis displacement data and the clear line presents the Y axis displacement data. First two graphics present in order the position and speed of the first tracking tests with an objective of 20 $\times$ . The third and fourth graphics show the second test results on a 50 $\times$  objective.

## 4. DISCUSSION & CONCLUSION

### 4.1 System characterization

We can observe in Fig. 4, a variation in the algorithm performance starting around 5500 pixels tested, which represents, in the user interface, a *search area radius* of approximately 37. Considering these results, and to optimize system performance, average *search area radius* should be kept below that limit. A higher value could imply missing some CCD frames.

Analysis of the maximum speed at which an object can be tracked gives us more information on the algorithm tracking behavior (Table 1). The test results show clearly a direct relation between the maximum speed at which a bacterium can be tracked and the ratio between the tracking window and bacterium size.

Analysis of the system configuration study leads to the conclusion that optimal system configuration for MTB tracking should be performed with a minimal object/search area ratio limiting the number of analyzed pixels underneath 5500. These factors should be taken into account when configuring the microscope parameters and CCD image resolution.

## 4.2 Bacteria tracking

Tracking and characterization of the bacteria was successfully realized. Better performance could be achieved using more CPU power. Parallel multi-task image analysis as well as Graphic Processor Unit (GPU) usage could be used to enhance performance. Evolution of the system through 3D tracking could benefit performance as well. Being able to follow a bacterium changing depth by adapting microscopic focus would allow longer tracking periods. Ensuring that the bacterium stays within the focus range could benefit tracking results as well.

Figure 5 allows observing variations in the readings linked to the microscope objective's force. We can clearly see that the results for speed will be impacted by the microscope configuration set-up. In this context, two situations may arise. The user can increase the size of the field of view which leads to a smaller size in pixel of the bacterium in the display. Such method is interesting for tracking over long distances but impacts the tracking quality by the possibility of losing the tracked object in size or confusing it with another one. The second approach is to use a smaller field of view where the bacterium appears bigger. This reduces the risk of losing the object being tracked, but can affect the algorithm performance at detecting the object's borders. The other problem arising with a smaller field of view comes from the fact that the possibility of losing track of the bacterium leaving the field of view is increased. Consequently, depending upon the characteristics of the objects being tracked; the field of view, lighting conditions and tracked area size as well as other parameters should be adjusted and considered before operating the system.

The tracking algorithm proved to be very efficient at following in real-time a bacterium attached to a bead. Main issues arose from confusion between two bacteria when superposition occurred and loss of the bacteria position when changing swimming depth. Other errors came from the change in color intensity of the bacterium moving at a higher speed. Once again, here, choosing the right objective and tracking parameters is critical.

Future progress could involve integrating magnetic control of the bacteria trajectory using microchips with an autonomous control system. Improvements to the software allowing tracking of swarms of bacteria could lead to interesting population statistical study as well.

## ACKNOWLEDGMENT

The authors acknowledge financial support from the Natural Sciences and Engineering Research Council of Canada (NSERC), the Canada Research Chair (CRC) in Micro/Nanosystem Development, Fabrication and Validation, the Canada Foundation for Innovation (CFI), and the Government of Québec. The authors would also like to thank Mahmood Mohammadi from the NanoRobotics Laboratory in assisting with biology-related issues related during the experiments.

## REFERENCES

1. S. Martel, "Targeted delivery of therapeutic agents with controlled bacterial carriers in the human blood vessels," In *2<sup>nd</sup> ASM/IEEE EMBS Conf. on Bio, Micro and Nanosystems*, San Francisco, USA, Jan. 15-18, 2006.
2. S. Martel, "Controlled bacterial micro-actuation," In *Proc. Int. Conf. on Microtechnologies in Medicine and Biology (MMB)*, Okinawa, Japan, 89-92, May 9-12, 2006
3. S. Martel, C. Tremblay, S. Ngakeng and G. Langlois, "Controlled manipulation and actuation of micro-objects with magnetotactic bacteria," *Appl. Phys. Lett.*, 89, 233804-6, 2006.
4. D. C. Fung and J. Theriot, "Imaging techniques in microbiology," *Curr. Opin. Microbiol.* 1(3), 346-51, 1998.